ACS Catalysis

Research Article

pubs.acs.org/acscatalysis

Electrochemical and Photoelectrochemical Water Oxidation by Supported Cobalt–Oxo Cubanes

Biaobiao Zhang,[†] Fei Li,*[,†] Fengshou Yu,[†] Xiaohong Wang,[†] Xu Zhou,[†] Hua Li,[†] Yi Jiang,[†] and Licheng Sun*[,†,‡]

[†]State Key Laboratory of Fine Chemicals, DUT-KTH Joint Education and Research Center on Molecular Devices, Dalian University of Technology (DUT), 116024 Dalian, China

[‡]Department of Chemistry, School of Chemical Science and Engineering, KTH Royal Institute of Technology, 100 44 Stockholm, Sweden

Supporting Information

ABSTRACT: Cobalt–oxo cubane clusters were immobilized on a Nafion film-coated fluorine-doped tin oxide (FTO) electrode and an α-Fe_2O_3 photoanode as surface catalysts for water oxidation. The performance of electrochemical water splitting indicated that these earth-abundant metal complexes retain their homogeneous reactivity on the electrode. Furthermore, efficient visible light-driven water oxidation was realized by coupling a molecular electrocatalyst with an inorganic semiconductor as a noble metal-free photoanode, showing a stability significantly improved with respect to that of the homogeneous system.

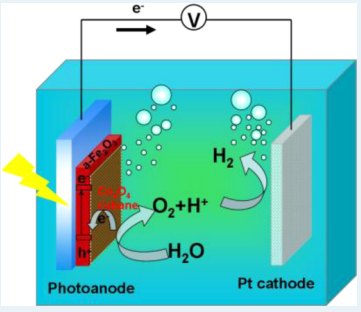

KEYWORDS: *cobalt–oxo cubane, photoanode, hematite, water splitting, oxygen evolution*

1. INTRODUCTION

Water oxidation plays a crucial role in artificial photosynthetic systems.[1] Recent advances demonstrate the advantages of synthetic molecular complexes serving as efficient water-splitting catalysts in terms of structural modification and mechanistic exploration. To date, the most active molecular catalysts with respect to water oxidation are dependent on expensive transition metals such as ruthenium and iridium.[2] To meet the criteria of producing large-scale renewable energy at low cost, earth-abundant metal complexes have attracted a great deal of attention,[3] among which the molecular tetracobalt cubane-shaped clusters, $Co_4O_4(O_2CMe)_4(py)_4$ (py = pyridine derivatives), are particularly attractive because of their cubical core that is structurally analogous to the oxygen-evolving complex (OEC) of photosystem II (PSII).[4−6] The photocatalytic activity of cobalt–oxo cubane for water oxidation has been reported by Dismukes[4] and Campagna[5] in homogeneous aqueous solutions consisting of a sacrificial electron acceptor, a photosensitizer, and a catalyst. In addition, Sartorel and co-workers have correlated the reactivity of cobalt–oxo cubane to the ligand substitution in the same system.[6] However, as a rare example of a water oxidation catalyst based on an earth-abundant metal,[7−13] the reactivity of cobalt–oxo cubane on a heterogeneous electrode aiming at applicable water splitting devices has not yet been explored. In this study, we report the electrochemical properties of cobalt–oxo cubanes modified on a fluorine-doped tin oxide (FTO) electrode as well as their photoelectrochemical (PEC) performance integrating with a visible light-absorbing semiconductor as a noble metal-free photoanode.

2. EXPERIMENTAL SECTION

Materials. FTO substrates were purchased from Dalian Heptachroma SolarTech Co., Ltd. (thickness of ~2.2 mm, transmittance of >90%, resistance of ~50 mΩ/cm^2). A Nafion 117 solution (5 wt % in lower aliphatic alcohols and water) was purchased from Sigma-Aldrich. Cobalt polyoxometalate $[Co_4(H_2O)_2(PW_9O_{34})_2]^{10-}$ was synthesized according to a reported procedure.[14] All other chemicals for the preparation of cobalt–oxo cubanes and α-Fe_2O_3 are commercially available, and all solvents were reagent grade and were dried prior to being used according to the standard methods.

Instruments. ^{1}H nuclear magnetic resonance (NMR) spectra were recorded at 298 K using a Bruker DRX-400 instrument operating at 400 MHz. Electrospray ionization mass spectra were recorded on a Q-Tof Micromass spectrometer (Manchester, England). UV–vis absorption measurements were taken with an Agilent 8453 spectrophotometer. Electrochemical and photoelectrochemical measurements were taken with a CHI660D electrochemical potentiostat. SEM micrographs and EDX analysis were conducted with a Nova NanoSEM 450 instrument with an accelerating voltage of 10.0 kV. X-ray diffraction was collected with a D/max-2400

Received: November 24, 2013
Revised: January 16, 2014
Published: January 27, 2014

diffractometer. Dynamic light scattering (DLS) measurements were performed on a DTS5101-type ZETASIZER1000 laser particle analyzer.

Synthesis of Cobalt–Oxo Cubanes. $Co^{III}_4(\mu_3\text{-}O)_4(\mu\text{-}O_2CCH_3)_4(4\text{-}CNpy)_4$ (**1-CN**),[15] $Co^{III}_4(\mu_3\text{-}O)_4(\mu\text{-}O_2CCH_3)_4(4\text{-}CH_3py)_4$ (**1-CH$_3$**),[16] and $Co^{III}_4(\mu_3\text{-}O)_4(\mu\text{-}O_2CCH_3)_4(4\text{-}CF_3py)_4$ (**1-CF$_3$**)[16] were prepared following the reported procedures. The characterizations of these complexes are indicated below. $Co^{III}_4(\mu_3\text{-}O)_4(\mu\text{-}O_2CCH_3)_4(4\text{-}CNpy)_4$ (**1-CN**): ^{1}H NMR (400 MHz, DMSO-d_6) δ 8.57 (d, J = 6.4 Hz, 8H), 7.70 (d, J = 6.8 Hz, 8H), 1.95 (s, 12H); ESI-MS m/z 953 $[M + H]^+$, 849 $[M - (4\text{-CNpy}) + H]^+$. $Co^{III}_4(\mu_3\text{-}O)_4(\mu\text{-}O_2CCH_3)_4(4\text{-}CH_3py)_4$ (**1-CH$_3$**): ^{1}H NMR (400 MHz, DMSO-d_6) δ 8.13 (d, J = 4.5 Hz, 8H), 6.96 (d, J = 4.4 Hz, 8H), 2.31 (s, 12H), 1.89 (s, 12H); ESI-MS m/z 909 $[M + H]^+$, 849 $[M - CH_3CO_2^-]^+$. $Co^{III}_4(\mu_3\text{-}O)_4(\mu\text{-}O_2CCH_3)_4(4\text{-}CF_3py)_4$ (**1-CF$_3$**): ^{1}H NMR (400 MHz, DMSO-d_6) δ 7.58 (d, J = 5.2 Hz, 8H), 8.66 (d, J = 5.2 Hz, 8H), 1.96 (s, 12H); ESI-MS m/z 1125 $[M + H]^+$, 1064 $[M - CH_3CO_2^-]^+$.

Fabrication of Cobalt–Oxo Cubane-Modified Composite Electrodes. The α-Fe_2O_3 electrodes used in this study were prepared according to the known method by electrodeposition of an iron film on a FTO substrate followed by annealing.[17] The obtained α-Fe_2O_3 film on FTO was characterized by scanning electronic microscopy (SEM), X-ray diffraction (XRD), and UV–vis spectroscopy, and the data were comparable to the related data reported previously.[17]

To fabricate cobalt–oxo cubane-modified electrodes, cubane complexes were dissolved in a 7:2:1 methanol/dichloromethane/Nafion mixture. The resulting solution contained 0.5% Nafion and 2 mM cobalt catalyst. A drop of solution (10 μL) was then casted onto the surface of the electrode (FTO or α-Fe_2O_3-coated FTO) and allowed to dry by evaporation. Finally, ~20 nmol of cobalt catalyst was loaded on the resulting electrode with an active area of 1.0 cm × 1.5 cm.

Electrochemical Measurements. Electrochemical experiments were taken in a three-electrode single-compartment cell. The cell was equipped with a FTO/Nafion/cobalt–oxo cubane electrode as the working electrode, a platinum wire as the counter electrode, and a Ag/AgCl (3.5 M KCl in water) reference electrode. Cyclic voltammetry and long-term controlled-potential electrolysis were conducted in pH 7 phosphate buffer (0.1 M) at ambient pressure and room temperature.

To determine the Faradaic efficiency,[18] the cell was sealed and purged with argon. An Ocean Optics oxygen sensor (FOXY-OR125-G) attached to a multifrequency phase fluorometer (MFPF-100) was fixed in the headspace of the cell. The kinetics of O_2 evolution was recorded with an oxygen sensor during electrolysis of the degassed phosphate buffer solution for 7 h. Upon termination of the electrolysis, the O_2 signal was recorded for an additional 2 h and the actual quantity of O_2 was determined by a GC 7890T instrument equipped with a thermal conductive detector. The theoretical amount of produced oxygen can be obtained by converting the charge passed into micromoles of gas according to Faraday's law. The Faradaic efficiency was calculated as O_2(actual)/O_2(theoretical) × 100%.

Photoelectrochemical Measurements. A similar three-electrode setup was used for photoelectrochemical measurements, where the cobalt–oxo cubane-modified α-Fe_2O_3 electrode was used as a photoanode. All photocurrent experiments were conducted in a pH 8 phosphate buffer (0.1 M) under visible light illumination using a 300 W Xe lamp (CEAULIGHT CEL-HXF300) through a cutoff filter (λ > 420 nm) to block ultraviolet light. The light intensity in front of the photoanode was 300 mW/cm^2 as measured by a CEAULIGHT CEL-NP2000 photometer. All films were irradiated from the front side of the photoanode, and the irradiated area was ~1.5 cm^2 for all experiments. Photocurrents were measured either by the way of linear sweeping voltammetry at a scan rate of 100 mV/s or under a constant bias (transient or long-term PEC) at ambient pressure and room temperature.

3. RESULTS AND DISCUSSION

The cubane-modified electrode used for electrochemical research was fabricated by dropping an MeOH/CH_2Cl_2/Nafion solution containing 20 nmol of **1-CN** (Figure 1) onto an FTO glass slide and allowed to dry at room temperature (see the details in the Supporting Information).[10]

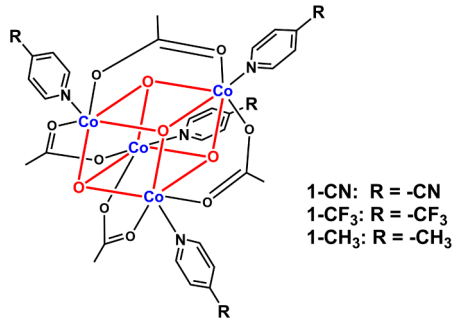

Figure 1. Representative structures of cobalt–oxo cubanes used in this study.

Cyclic voltammograms (CVs) in Figure 2a reveal that a cobalt–oxo cubane-doped Nafion film is catalytically active to oxygen evolution. In pH 7 phosphate buffer, a sharply increased current wave was observed after the potential passed 1.0 V (all potentials are vs Ag/AgCl), which is attributed to water oxidation as compared with the electrode in the absence of a supported cobalt complex. To explore the robustness of the **1-CN**-modified electrode, long-term controlled-potential electrolysis (CPE) was conducted using a single-compartment cell processing a FTO/Nafion/1-CN working electrode, a Pt counter electrode, and a Ag/AgCl reference electrode. As shown in Figure 2b, a stable current density of 230 μA/cm^2 persists for 10 h in neutral phosphate buffer under an applied potential of 1.2 V. Taking into account the fact that the bare FTO/Nafion electrode shows a much lower current under the same conditions (Figure 2b), we believe the significant improvement in current density is induced by a surface catalyst. Using a fluorescent oxygen sensor fixed in the headspace of the cell, it was found that 44 μmol of O_2 was produced by electrolysis, in accord with a Faradaic efficiency of 95% and fitting well the ideal oxygen evolution by assuming that all charge was consumed for O_2 production (Figure S1 of the Supporting Information). The Tafel plot of the composite electrode is shown in Figure S2 of the Supporting Information. Similar to that shown by cobalt hangman corrle embedded in Nafion,[10] a slope of 120 mV/decade indicates that electron transfer is the rate-determining step.

Identification of the real catalytic active species is an important issue. Some homogeneous catalysts were found to convert to heterogeneous nanoparticles, which is responsible

dx.doi.org/10.1021/cs401109u | ACS Catal. 2014, 4, 804–809

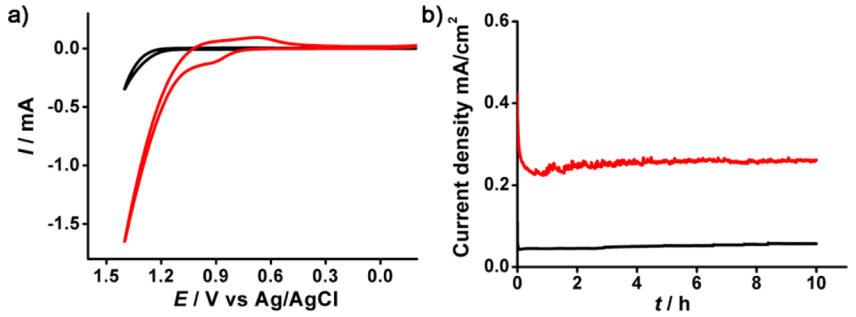

Figure 2. (a) Cyclic voltammograms of the blank FTO/Nafion (black) and **1-CN**-doped FTO/Nafion (red) electrodes in pH 7 phosphate buffer recorded with a scan rate of 100 mV/s. (b) Controlled-potential electrolyses of FTO/Nafion (black) and **1-CN**-doped FTO/Nafion (red) electrodes in pH 7 phosphate buffer at 1.2 V vs Ag/AgCl.

for oxygen evolution.[19−21] For example, Mn_4O_4 cubane doped in Nafion was recently evidenced to be the precursor of manganese oxide, which is the active species for the observed photoinduced water oxidation.[22] Nevertheless, Dismukes and Scandola indicated that cobalt−oxo cubanes remain intact during homogeneous photocatalytic water oxidation.[4,5] The experimental results of this system basically agree with their assumption. (i) CVs of **1-CN** before and after electrolysis in Figure 3a were found to be essentially unchanged; the FTO

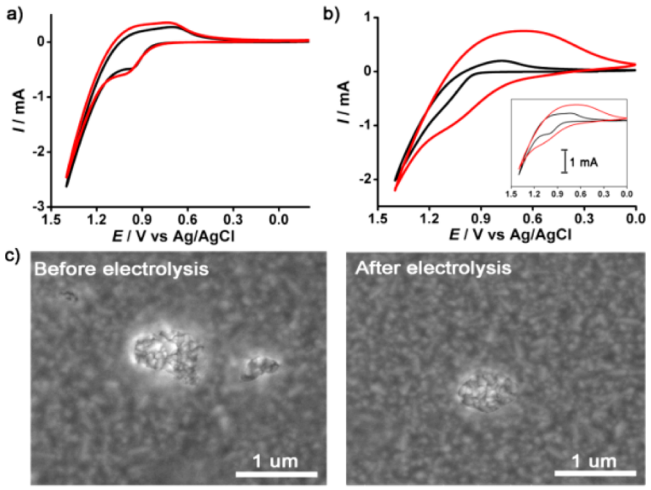

Figure 3. (a) Cyclic voltammograms of the **1-CN**-doped FTO/Nafion electrode before (black) and after (red) electrolysis for 10 h (1.2 V, pH 7 phosphate buffer, scan rate of 100 mV/s). (b) Cyclic voltammograms of the $Co(NO_3)_2$-doped FTO/Nafion electrode before (black) and after (red) electrolysis for 10 h (1.2 V, pH 7 phosphate buffer, scan rate of 100 mV/s). The inset shows a comparison of the CVs of $Co(NO_3)_2$-doped (red) and **1-CN**-doped (black) FTO/Nafion electrodes after electrolysis. (c) SEM images of the **1-CN**-doped FTO/Nafion electrode before and after electrolysis.

electrode rinsed with methanol after electrolysis showed no catalytic activity toward water oxidation, and no deposition was observed on the surface of FTO. The resulting methanol solution was concentrated and examined by UV−vis spectrometry (Figure S3 of the Supporting Information), exhibiting characteristics identical to those of the initial solution used for electrode casting. (ii) Dynamic light scattering (DLS) revealed no colloidal particles present in the initial MeOH/CH_2Cl_2/Nafion solution. (iii) The scanning electron microscopy (SEM) image in Figure 3c discloses that the electrode is covered by a layer of a catalyst-doped Nafion film with small holes. The morphology of the Nafion film was not changed by electrolysis. In comparison, the Mn_4O_4 cubane was found to form manganese oxide nanoparticles under a given applied potential.[22] (iv) Because no metal oxide was found, **1-CN** dispersed in the Nafion layer was tested by mass spectrometry (Figure S4 of the Supporting Information). The domain signals in the ESI-MS spectra were found to be identical before and after electrolysis. Considering that **1-CN** is a coordination saturation complex and the appearance of the signal at m/z 848 due to $[M - 4\text{-CNpy} + H]^+$, it is possible that one pyridine ligand of **1-CN** may exchange with water to initiate the catalysis.

In spite of challenges in distinguishing homogeneous and heterogeneous water oxidation, for example, the fact that nanomolar metal oxide formed from micromolar molecular precursors may account for the observed O_2 evolution, obvious differences were displayed by comparing the electrochemical behavior of **1-CN** with that of cobalt complexes those were known to be precursors of cobalt oxide both in Nafion and in solution. For example, unlike that of **1-CN**, the CV of $Co(NO_3)_2$ embedded in Nafion was found to be dramatically altered by electrolysis (Figure 3b), whose shape is quite similar to that of Nocera's cobalt phosphate thin film (CoP_i).[23] The Co^{2+}-functionalized electrode after electrolysis was rinsed with methanol. The resulting electrode remained active toward water oxidation and produced substantial current density at a given voltage. Meanwhile, a considerable enhancement of phosphorus content was found by energy dispersive X-ray analysis (EDX), reaching a P:Co ratio of 1:2. Thus, the CoP_i compound was thought to deposit on the FTO surface (Figure S5 of the Supporting Information).[24] In contrast, negligible P was detected for FTO/Nafion/**1-CN** through the course of electrolysis.

Tetracobalt polyoxometalate $[Co_4(H_2O)_2(PW_9O_{34})_2]^{10-}$ was recently reported to convert to cobalt oxide during electrolysis in a neutral homogeneous solution.[19] Thus, the electrochemical behavior of **1-CN** was compared with that of $[Co_4(H_2O)_2(PW_9O_{34})_2]^{10-}$ by performing CPEs in phosphate buffers (0.1 M, pH 7) with an added cobalt complex at a concentration of 1.25×10^{-4} M (Figure 4a). Consistent with Finke's report,[19] a layer of cobalt oxide formed on FTO accompanied by a steady increase in the current density in the solution containing cobalt polyoxometalate. The buffer containing cobalt−oxo cubane, however, shows negligible catalytic current after electrolysis for 3 h. Furthermore, both FTO electrodes after electrolysis were rinsed with water and examined in fresh aqueous buffers without catalyst. As shown in Figure 4b, the CV of the electrode removed from the cobalt

dx.doi.org/10.1021/cs401109u | ACS Catal. 2014, 4, 804−809

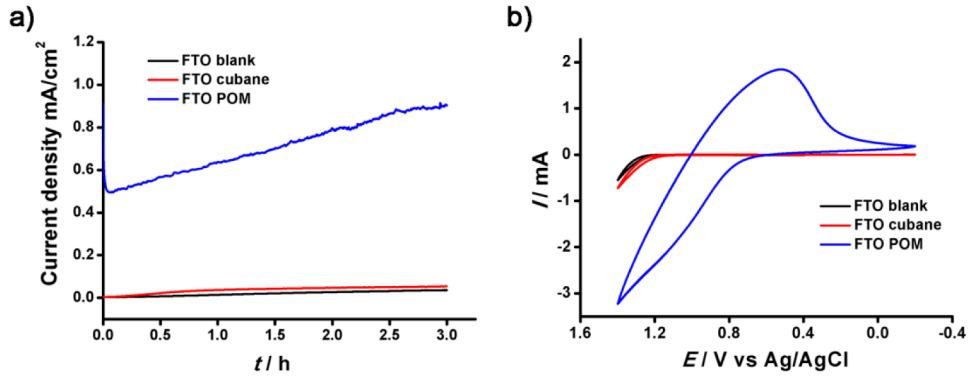

Figure 4. (a) Controlled-potential electrolyses of the phosphate buffer solutions (0.1 M, pH 7) of **1-CN** (red) and cobalt polyoxometalate (blue) at a concentration of 1.25×10^{-4} M at 1.2 V vs Ag/AgCl. CH_3CN (10% in volume) was added to the buffer solution containing **1-CN** because of its poor water solubility. (b) Cyclic voltammograms of the FTO electrodes removed from the CPE solutions containing **1-CN** (red) and cobalt polyoxometalate (blue). The electrodes were rinsed with water before CV analysis in phosphate buffers (0.1 M, pH 7).

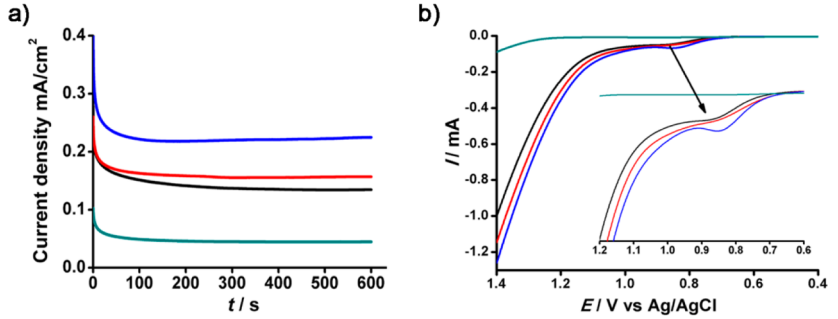

Figure 5. (a) Steady-state current densities at 1.2 V vs Ag/AgCl and (b) liner sweep voltammograms of **1-CH_3**-doped (black), **1-CF_3**-doped (red), **1-CN**-doped (blue), and $[Co(bpy)_2(H_2O)_2](ClO_4)_2$-doped (green) electrodes in a pH 7 phosphate buffer solution.

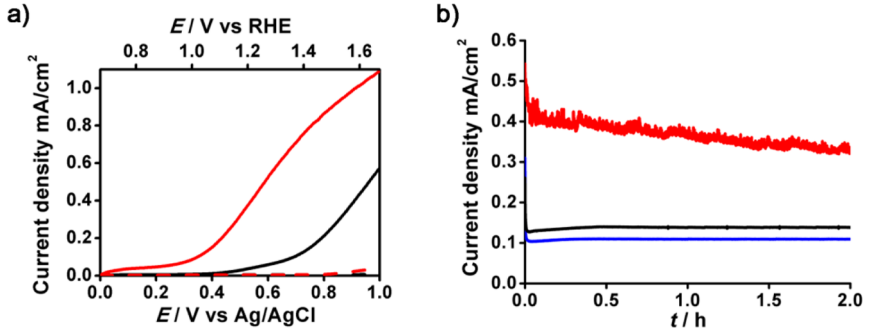

Figure 6. (a) Photocurrent–potential characteristics in the dark (dashed lines) and under visible light illumination (300 mW/cm^2) (solid lines) for α-Fe_2O_3/Nafion (black) and α- Fe_2O_3/Nafion/**1-CN** (red) photoanodes in a pH 8 phosphate buffer solution. (b) Long-term photocurrent densities of α-Fe_2O_3 (black), α-Fe_2O_3/Nafion (blue), and α-Fe_2O_3/Nafion/**1-CN** (red) photoanodes obtained at a bias of 0.6 V vs Ag/AgCl in a pH 8 phosphate buffer solution under visible light illumination (300 mW/cm^2).

polyoxometalate solution shows a large catalytic current because of surface-deposited species. In contrast, the CV of the electrode removed from the **1-CN** solution essentially overlaps the background of naked FTO. Though we could not completely exclude the presence of metal oxide, the molecular species was assumed to play a key role in catalysis on the basis of the observations described above.

We have gained further insight into the impact of ligand modification on electrochemical water oxidation by varying the substituent on the pyridine ligand of **1**. The steady-state currents were observed to depend strongly on ligands and increase in the following order: **1-CH_3** < **1-CF_3** < **1-CN** (Figures 1 and 5a). Moreover, upon replacement of the cubic core by mononuclear $[Co(bpy)_2(H_2O)_2]^{2+}$ (bpy = 2,2′-bipyridine), the catalytic current significantly decreased to one-fourth of that for **1-CN** (Figure 5a). This reactivity trend correlates well with the onset potential and the magnitude of the catalytic current of the individual complex shown by linear sweep voltammetry (Figure 5b), highlighting the unique role of subtle structures on tuning catalytic activities. All these findings demonstrate cobalt–oxo cubanes are a family of competent molecular electrocatalysts.

Having these results in hands, we decided to explore the photocatalytic properties of cobalt–oxo cubane on a heterogeneous surface. Generally, the poor stability of organic and organometallic photosensitizers in a homogeneous system greatly limits the overall photocatalytic performance of the water-splitting catalysts. For example, popularly used [Ru-

dx.doi.org/10.1021/cs401109u | ACS Catal. 2014, 4, 804–809

$(bpy)_3]^{2+}$ suffers from photodecomposition in aqueous solutions.[25] On the other hand, some n-type semiconductors are photostable materials possessing suitable band gaps for visible light absorption in spite of slow oxygen-evolving reaction kinetics. A major effort to improve the efficiency of a semiconductor is to couple it with an appropriate electrocatalyst to facilitate the kinetics and reduce overpotentials for water oxidation.[26] For instance, highly efficient composite photoanodes were developed by electro- or photoelectrodeposition of a metal oxide such as IrO_2, a "Co-P_i" catalyst on hematite (α-Fe_2O_3).[27] Therefore, it would be valuable to build a robust solar water-splitting system by combining an inorganic semiconductor and a molecular catalyst. As a proof of concept, **1-CN** was immobilized on hematite to form a combined photoanode in a PEC cell; we anticipated that the photogenerated holes in hematite would drive water oxidation by the supported catalyst.

The α-Fe_2O_3 film was prepared according to a known procedure of Choi et al. and showed characteristics similar to those reported previously (Figures S6–S9 of the Supporting Information).[28] The composite photoanode was fabricated following the method for the FTO/Nafion/**1-CN** photoanode except that the FTO substrate was replaced with α-Fe_2O_3-coated FTO. The PEC performance was measured in a three-electrode single-compartment cell with the composite photoanode as the working electrode, Ag/AgCl as the reference electrode, and Pt as the counter electrode. Figure 6a shows dark currents and photocurrents of different photoanodes in pH 8 phosphate buffer under visible light illumination. Notably, the **1-CN**-modified photoanode leads to a significant cathodic shift of onset potential for water oxidation by 400 mV as compared with that of the Nafion-coated α-Fe_2O_3 or bare α-Fe_2O_3 (Figure S10 of the Supporting Information). At a given bias, the composite photoanode achieves substantially enhanced photocurrent density with respect to the photoanode without catalyst modification. For example, the transient photocurrent for α-Fe_2O_3 at a bias of 0.5 V versus Ag/AgCl was increased as much as 6-fold to 200 $\mu A/cm^2$ when the composite photoanode was applied (Figure S11 of the Supporting Information). Although the lifetimes for solar water oxidation systems using organometallic photosensitizers are normally limited to <1 h,[4,12,21b,25,29,30] the α-Fe_2O_3/Nafion/**1-CN** photoanode exhibits considerable stability against photodecomposition. As shown in Figure 6b, a steady photocurrent is maintained above 350 $\mu A/cm^2$ under extended periods of illumination at 0.6 V. During this experiment, the O_2 and H_2 produced from water splitting were monitored by GC to keep a standard ratio of 1:2. The slight decay of photocurrent is due to oxygen bubbles that accumulated on the electrode surface, which may decrease the number of active sites for the reaction. However, the initial photocurrent could be simply recovered by removing the gas bubbles on the electrode (Figure S12 of the Supporting Information), and the photoanode was allowed to be used repeatedly. The stability of **1-CN** on the photoanode was confirmed by CV and UV–vis absorption measurement, both of which showed identical features before and after light irradiation (Figures S13 and S14 of the Supporting Information).

Despite preliminary results, the findings described above indicate that modification of cobalt–oxo cubane on the surface of α-Fe_2O_3 is capable of combining the merits of both an inorganic photosensitizer and a synthetic catalyst and is a promising approach to a robust PEC device.

4. CONCLUSION

In summary, we have shown that the supported cobalt–oxo cubanes are robust and efficient electrocatalysts as molecular mimics of the OEC. The evidence obtained so far suggests the molecular identity of the catalytic active species on the electrode. Cobalt–oxo cubane was further integrated with α-Fe_2O_3 as a composite photoanode in PEC, which significantly shifts the onset potential for water oxidation and greatly enhances the photocurrent. To the best of our knowledge, this is the first time to achieve water oxidation by a combination of an inorganic semiconductor and a noble metal-free molecular catalyst.[31] The development of more efficient PEC cells containing low-cost molecular complexes is ongoing.

■ ASSOCIATED CONTENT

Supporting Information

UV–vis, ESI-MS, and EDX spectra and photoelectrochemical measurement data. This material is available free of charge via the Internet at http://pubs.acs.org.

■ AUTHOR INFORMATION

Corresponding Authors

*E-mail: lifei@dlut.edu.cn.
*E-mail: lichengs@kth.se.

Notes

The authors declare no competing financial interest.

■ ACKNOWLEDGMENTS

This work was supported by the National Basic Research Program of China (973 program) (2014CB239402), the National Natural Science Foundation of China (21106015, 21120102036, and 21361130020), the Research Fund for the Doctoral Program of Higher Education of China (20110041120005), the Swedish Energy Agency, and the K&A Wallenberg Foundation.

■ REFERENCES

(1) (a) Rüttinger, W.; Dismukes, G. C. *Chem. Rev.* **1997**, *97*, 1–24. (b) Lewis, N. S.; Nocera, D. G. *Proc. Natl. Acad. Sci. U.S.A.* **2006**, *103*, 15729–15735.

(2) (a) Sala, X.; Romero, I.; Rodríguez, M.; Escriche, L.; Llobet, A. *Angew. Chem., Int. Ed.* **2009**, *48*, 2842–2852. (b) Cao, R.; Lai, W.; Du, P. *Energy Environ. Sci.* **2012**, *5*, 8134–8157. (c) Duan, L.; Tong, L.; Xu, Y.; Sun, L. *Energy Environ. Sci.* **2011**, *4*, 3296–3313. (d) Hetterscheid, D. G. H.; Reek, J. N. H. *Angew. Chem., Int. Ed.* **2012**, *51*, 9740–9747.

(3) Du, P.; Eisenberg, R. *Energy Environ. Sci.* **2012**, *5*, 6012–6021.

(4) McCool, N. S.; Robinson, D. M.; Sheats, J. E.; Dismukes, G. C. *J. Am. Chem. Soc.* **2011**, *133*, 11446–11449.

(5) Ganga, G. L.; Puntoriero, F.; Campagna, S.; Bazzan, I.; Berardi, S.; Bonchio, M.; Sartorel, A.; Natali, M.; Scandola, F. *Faraday Discuss.* **2012**, *155*, 177–190.

(6) Berardi, S.; Ganga, G. L.; Natali, M.; Bazzan, I.; Puntoriero, F.; Sartorel, A.; Scandola, F.; Campagna, S.; Bonchio, M. *J. Am. Chem. Soc.* **2012**, *134*, 11104–11107.

(7) Ellis, W. C.; McDaniel, N. D.; Bernhard, S.; Collins, T. J. *J. Am. Chem. Soc.* **2010**, *132*, 10990–10991.

(8) Fillol, J. L.; Codolà, Z.; Garcia-Bosch, I.; Gómez, L.; Pla, J. J.; Costas, M. *Nat. Chem.* **2011**, *3*, 807–813.

(9) Yin, Q.; Tan, J. M.; Besson, C.; Geletti, Y. V.; Musaev, D. G.; Kuznetsov, A. E.; Luo, Z.; Hardcastle, K. I.; Hill, C. L. *Science* **2010**, *328*, 342–345.

(10) Dogutan, D. K., Jr.; McGuire, R.; Nocera, D. G. *J. Am. Chem. Soc.* **2011**, *133*, 9178–9180.

(11) Wasylenko, D. J.; Ganesamoorthy, C.; Borau-Garcia, J.; Berlinguette, C. P. *Chem. Commun.* **2011**, *47*, 4249−4251.
(12) Leung, C.-F.; Ng, S.-M.; Ko, C.-C.; Man, W.-L.; Wu, J.-S.; Chen, L.-J.; Lau, T.-C. *Energy Environ. Sci.* **2012**, *5*, 7903−7907.
(13) Barnett, S. M.; Goldberg, K. I.; Mayer, J. M. *Nat. Chem.* **2012**, *4*, 498−502.
(14) Finke, R. G.; Droege, M. W.; Domaille, P. J. *Inorg. Chem.* **1987**, *26*, 3886−3896.
(15) Chakrabarty, R.; Kalita, D.; Das, B. K. *Polyhedron* **2007**, *26*, 1239−1244.
(16) Chakrabarty, R.; Bora, S. J.; Das, B. K. *Inorg. Chem.* **2007**, *46*, 9450−9462.
(17) McDonald, K. J.; Choi, K.-S. *Chem. Mater.* **2011**, *23*, 1686−1693.
(18) Li, F.; Zhang, B.; Li, X.; Jiang, Y.; Chen, L.; Li, Y.; Sun, L. *Angew. Chem., Int. Ed.* **2011**, *50*, 12276−12279.
(19) Stracke, J. J.; Finke, R. G. *J. Am. Chem. Soc.* **2011**, *133*, 14872−14875.
(20) Blakemore, J. D.; Schley, N. D.; Olack, G. W.; Incarvito, C. D.; Brudvig, G. W.; Crabtree, R. H. *Chem. Sci.* **2011**, *2*, 94−98.
(21) (a) Hong, D.; Murakami, M.; Yamada, Y.; Fukuzumi, S. *Energy Environ. Sci.* **2012**, *5*, 5708−5716. (b) Hong, D.; Jung, J.; Park, J.; Yamada, Y.; Suenobu, T.; Lee, Y.-M.; Nam, W.; Fukuzumi, S. *Energy Environ. Sci.* **2012**, *5*, 7606−7616.
(22) Hocking, R. K.; Brimblecombe, R.; Chang, L.-Y.; Singh, A.; Cheah, M. H.; Glover, C.; Casey, W. H.; Spiccia, L. *Nat. Chem.* **2011**, *3*, 461−466.
(23) Ahn, H. S.; Tilley, T. D. *Adv. Funct. Mater.* **2013**, *23*, 227−233.
(24) Kanan, M. W.; Nocera, D. G. *Science* **2008**, *321*, 1072−1075.
(25) Geletii, Y. V.; Huang, Z.; Hou, Y.; Musaev, D. G.; Lian, T.; Hill, C. L. *J. Am. Chem. Soc.* **2009**, *131*, 7522−7523.
(26) (a) Zhong, D. K.; Sun, J.; Inumaru, H.; Gamelin, D. R. *J. Am. Chem. Soc.* **2009**, *131*, 6086−6087. (b) Steinmiller, E. M. P.; Choi, K.-S. *Proc. Natl. Acad. Sci. U.S.A.* **2009**, *106*, 20633−20636. (c) Seabold, J. A.; Choi, K.-S. *J. Am. Chem. Soc.* **2012**, *134*, 2186−2192. (d) Barroso, M.; Cowan, A. J.; Pendlebury, S. R.; Grätzel, M.; Klug, D. R.; Durrant, J. R. *J. Am. Chem. Soc.* **2011**, *133*, 14868−14871.
(27) For metal oxide-modified hematite photoanode, see the review: Sivula, K.; Formal, F. L.; Grätzel, M. *ChemSusChem* **2011**, *4*, 432−449 and references cited therein.
(28) McDonald, K. J.; Choi, K.-S. *Chem. Mater.* **2011**, *23*, 1686−1693.
(29) Tanaka, S.; Annaka, M.; Sakai, K. *Chem. Commun.* **2012**, *48*, 1653−1655.
(30) Karlsson, E. A.; Lee, B.-L.; Åkermark, T.; Johnston, E. V.; Kärkäs, M. D.; Sun, J.; Hansson, Ö.; Bäckvall, J.-E.; Åkermark, B. *Angew. Chem., Int. Ed.* **2011**, *50*, 11715−11718.
(31) Molecular ruthenium WOCs were reported to be modified on hematite and WO_3: (a) Chen, X.; Ren, X.; Liu, Z.; Zhuang, L.; Lu, J. *Electrochem. Commun.* **2013**, *27*, 148−151. (b) Zhong, D. K.; Zhao, S.; Polyansky, D. E.; Fujita, E. *J. Catal.* **2013**, *307*, 140−147.